Sensors and Actuators B 190 (2014) 32–39

Contents lists available at ScienceDirect

Sensors and Actuators B: Chemical

journal homepage: www.elsevier.com/locate/snb

One-step synthesis and gas sensing properties of hierarchical Cd-doped SnO_2 nanostructures

Peng Sun[a], Xin Zhou[a], Chen Wang[a], Biao Wang[b], Xiumei Xu[a], Geyu Lu[a,*]

[a] State Key Laboratory on Integrated Optoelectronics, College of Electronic Science and Engineering, Jilin University, Changchun 130012, People's Republic of China

[b] State Key Laboratory of Luminescence and Application, Changchun Institute of Optics, Fine Mechanics and Physics, Chinese Academy of Science, Changchun 130033, People's Republic of China

ARTICLE INFO

Article history:
Received 28 January 2013
Received in revised form 12 August 2013
Accepted 13 August 2013
Available online 28 August 2013

Keywords:
Cd-doped SnO_2
Hydrothermal method
Nanorod
Gas sensor

ABSTRACT

The hierarchical undoped and Cd-doped SnO_2 nanostructures had been synthesized via a low-cost and environmentally friendly hydrothermal route. The morphology and structure of the as-prepared product were characterized by X-ray diffraction (XRD), field-emission electron microscopy (FESEM), and transmission electron microscopy (TEM). The images of field-emission electron microscopy and transmission electron microscopy showed that pure and Cd-doped SnO_2 hierarchical architectures were built from one-dimensional nanorods. X-ray diffraction (XRD) of the doped samples revealed that Cd incorporation led to lattice deformation without destroying the original crystal structure. Gas sensors based on undoped and Cd-doped SnO_2 nanorods were fabricated, and their gas sensing properties were tested for various gases. The 3.0 wt% Cd-doped SnO_2 based sensor showed excellent selectivity toward H_2S at the operating temperature 275 °C, giving a response of about 31–10 ppm, which was about 22 times higher than that of sensor based on pure SnO_2.

1. Introduction

The investigation of gas sensors has received considerable attention in recent years, due to their profound influence on personal safety, medical diagnosis, detection of pollutants and toxins, and the transportation industries [1,2]. It is well known that performances of gas sensors are regulated by their sensitivity, selectivity, response/recovery speed, stability and reproducibility. Therefore, new sensor strategies for ever increasing sensitivity, selectivity, and reduction of cost seem to be constant in demand [3–9]. Due to their high sensitivity to the target gases and simplicity in preparation, metal-oxide semiconductors such as SnO_2, α-Fe_2O_3, ZnO, and In_2O_3 have been extensively investigated as sensing materials in the past ten years. Previous researches have showed that the gas sensing properties of oxide semiconductors were closely related with their composition, crystalline size, and surface morphology. Many studies have been conducted in order to improve the performance of gas sensors by using crystallites with reduced dimensions since Yamazone demonstrated that a reduction in crystallite size could significantly increase sensor performance [10]. However, the aggregation between the nanoparticles will result in the degradation of the gas sensing properties [11–13]. Recently, metal-oxide semiconductors with hierarchical structures, higher dimension of a microstructure or nanostructure assembled from low dimensional nanosized building blocks, have been demonstrated to be promising candidates for ultrasensitive sensors due to their low density, large surface area, and surface permeability.

Tin dioxide (SnO_2), a well-known n-type wide band gap semiconductor (E_g = 3.6 eV, at 300 K), is considered as the most promising sensing material for a gas sensor for the detection of a wide variety of pollutant gases owing to its attractive features including low cost, nontoxicity, and simple preparation [14,15]. Although exciting results have been reported, the development of more highly sensitive and markedly selective gas sensors based on hierarchical SnO_2 nanostructures remains a challenge. It is well known that the sensing mechanism of SnO_2 belongs to the surface-controlled type, in which the grain size, defect, and oxygen-adsorption quantity play important roles in sensing properties. Nowadays, in order to meet the increasing demands for making sensors work in more complicated systems and under more harsh conditions, many efforts have been taken such as element doping, heterostructure constructing, and adding catalyst [16–22]. Among these methods, doping has been reported to be a very simple and feasible way to enhance the gas sensing properties of SnO_2 via altering its structure and grain size or introducing an impurity level and surface defects [23]. Markedly enhanced sensing properties have been obtained by doping transition metals in SnO_2 nanostructures. For instance, Cu, Ni, and Zn have been known to promote

* Corresponding author. Tel.: +86 431 85167808; fax: +86 431 85167808.
E-mail addresses: lugy@jlu.edu.cn, spmaster2008@163.com (G. Lu).

0925-4005/$ – see front matter © 2013 Elsevier B.V. All rights reserved.
http://dx.doi.org/10.1016/j.snb.2013.08.045

the sensitivity, selectivity, and response speed of SnO_2 to specific gases [24–27]. Recently, it has been reported that the gas sensing properties of SnO_2 can be improved by Cd doping due to the substitution of Cd^{2+} for Sn^{4+} may possibly result in more oxygen vacancies for charging compensation [28–30]. However, to the best of our knowledge, studies of Cd-doped SnO_2 hierarchical nanostructures obtained by a simple hydrothermal route have rarely been reported.

In this paper, we present a facile hydrothermal method for the synthesis of the hierarchical undoped and Cd-doped SnO_2 nanostructures. The obtained SnO_2 hierarchical nanostructures consisted of a number of one-dimensional (1D) nanorods. Moreover, to demonstrate the potential applications, the gas-sensing properties of as-prepared SnO_2 hierarchical nanostructures were investigated. A comparative gas sensing study between the Cd-doped SnO_2 and pure SnO_2 hierarchical architectures was performed to demonstrate the superior gas sensing properties of the hierarchical Cd-doped SnO_2 nanorods. As expected, the sensor using 3.0 wt% Cd-doped SnO_2 nanorods displayed good selectivity and high response to H_2S. It was found that the sensor had a response of 31–10 ppm H_2S, which was about 22 times higher than that of the pure SnO_2 nanorods at the same operating temperature (275 °C).

2. Experimental

2.1. Synthesis and characterization of hierarchical Cd-doped SnO_2

A series of Cd-doped SnO_2 (0.0 wt%, 1.0 wt%, 3.0 wt%, and 5.0 wt%) hierarchical architectures were synthesized by hydrothermal reaction. All the chemical reagents were purchased from Beijing Chemical Co. and used as received without further purification, $SnCl_4{\cdot}5H_2O$ and $Cd(NO_3)_2{\cdot}4H_2O$ were used as tin and cadmium sources, respectively. In a typical synthesis process, $SnCl_4{\cdot}5H_2O$ (0.526 g), cetyltrimethyl ammonium bromide (CTAB 0.6 g), hexamethylenetetramine (HMT 0.2 g) were added to 40 cm^3 basic mixture of ethanol and water (1:1, v/v) with vigorous stirring. Then an appropriate amount of $Cd(NO_3)_2{\cdot}4H_2O$ was added to the above solution. After 30 min stirring, the mixture was transferred into a Teflon-lined stainless-steel autoclave and maintained at 200 °C for 24 h. After the hydrothermal procedure, the autoclave cooled naturally down to room temperature. The resultant precipitates were centrifuged, washed with distilled water and absolute ethanol, and dried at 80 °C.

The X-ray diffraction (XRD) patterns were recorded on a Rigaku TTRIII X-ray diffractometer with Cu Kα1 radiation (λ = 1.5406 Å), field emission scanning electron microscopy (FESEM) images were obtained using a JEOL JSM-7500F microscope with an acceleration voltage of 15 kV. The energy dispersive X-ray spectrometry (EDS) result was measured by the FESEM attachment. Transmission electron microscopic (TEM), high-resolution transmission electron microscopic (HRTEM) images, and selected-area electron diffractive (SAED) patterns were obtained on a JEOL JEM-3010 transmission electron microscope with an acceleration voltage of 200 kV.

2.2. Fabrication and measurement of gas sensor

Gas sensors were fabricated as follows: the prepared products were mixed with deionized water to form paste, and then coated on an alumina tube (4 mm in length, 1.2 mm in external diameter, and 0.8 mm in internal diameter, attached with a pair of gold electrodes) by a small brush to form a thick film, and the detailed fabrication has been described in the literatures [31,32]. The sensing properties of the sensors were determined using a RQ-2 gas-sensing characterization system under laboratory conditions. The measurement was processed by a static process: first, fresh air (atmospheric air) was introduced into a closed glass chamber, and then a given amount of the tested gas was injected into the chamber by a microinjector, and the sensor was put into the chamber for the measurement of the sensitive performance. The desired concentration of the VOC gas was obtained by the static liquid gas distribution method, which was calculated by the following formula [33]:

$$C = \frac{22.4 \times \varphi \times \rho \times V_1}{M \times V_2} \times 1000 \quad (1)$$

where C (ppm) is the target gas concentration, φ the required gas volume fraction, ρ (g/mL) the density of the liquid, V_1 (μL) the volume of liquid, V_2 (L) the volume of the chamber, and M (g/mol) the molecular weight of the liquid. The response of sensor was defined as the ratio of the resistance of the sensor in air (R_a) to that in tested gas atmosphere (R_g). The response time and recovery time were defined as the times taken by the sensor to achieve 90% of the total resistance changes in the case of adsorption and desorption processes, respectively.

3. Results and discussion

The morphologies and microstructures of the obtained SnO_2 products were characterized by FESEM. A panoramic FESEM image of the hierarchical undoped SnO_2 nanorods obtained after hydrothermal treatment at 200 °C for 24 h (Fig. A1a, supplementary materials) shows that a number of flower-like structures with an average diameter of 2 μm were clearly observed. No other morphologies could be detected, indicating a high yield of these 3D microstructures. It can be seen from the enlarged FESEM image of Fig. 1a that the products were composed of uniform nanorods with diameters of 100–150 nm and the lengths of 400–500 nm. The morphologies of the Cd-doped samples are shown in Fig. 1b–d. Comparison of the images before and after doped clearly finds that the morphologies of products were similar (Fig. A1b, supplementary materials), but by increasing the Cd doping amount, the sizes of as-prepared SnO_2 nanostructures gradually decreased, which probably resulted from suppressing grain boundary migration and increasing the energy barrier for grain growth [34]. The EDX analysis (Fig. A2, supplementary materials) reveals that the composition of hierarchical architectures (3.0 wt% Cd-doped SnO_2) consisted of Sn, Cd and O elements. Besides, the Si element signal in the spectrum was attributed to the substrate used to support the sample.

Fig. 2a shows the XRD pattern of the as-synthesized products. For undoped sample, all of the diffraction peaks can be indexed to tetragonal rutile structure of SnO_2. This was in good agreement with the JCPDS file of SnO_2 (JCPDS 41-1445). For the as-prepared Cd-doped SnO_2 (1.0 and 3.0 wt%) hierarchical architectures, no other crystalline phase and obvious peaks of impurities were detected in Fig. 2a. The results indicated that Cd could be incorporated into the lattice of SnO_2. However, for 5.0 wt% Cd-doped sample, diffraction peaks corresponding to the $CdSnO_3$ were observed. The relative intensity of the diffraction deviated from that of the bulk, showing the anisotropic growth of the Cd-doped SnO_2 nanorods [35]. To investigate the effect of doping on the crystallinity of the SnO_2 nanorods, the (1 1 0) and (1 0 1) diffraction peaks were monitored. Fig. 2b displays that there was 0.1° left shift in both (1 1 0) and (1 0 1) diffraction peaks of 3.0 wt% Cd-doped SnO_2 compared with those of pure SnO_2. This proved that Cd incorporation led to lattice deformation in the doped SnO_2. However, no characteristic peaks of CdO or $CdSnO_3$ were observed for 3.0 wt% Cd-doped SnO_2. All of these indicated that Cd ions systematically entered the crystal lattice of SnO_2 nanorods without deteriorating the original crystal structure.

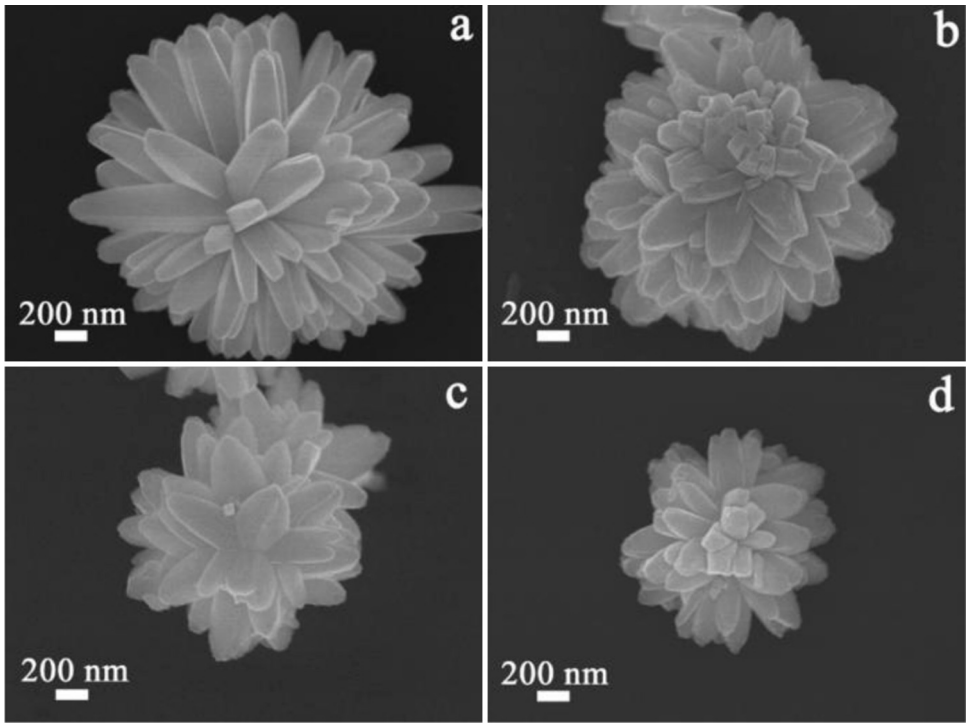

Fig. 1. FESEM images of (a) unloaded SnO_2 nanorods. Cd-doped SnO_2 nanorods obtained with different amount of Cd (b) 1.0 wt%, (c) 3.0 wt%, and (d) 5.0 wt%.

Here, we evaluated the lattice constants a and c of pure and doped SnO_2 according to Bragge's law

$$n\lambda = 2d \sin\theta \tag{2}$$

In Eq. (1) n is the order of diffraction (usually $n = 1$), λ is the X-ray wavelength, and d is the spacing between planes of given Miller indices h, k, and l. In the tetragonal structure of SnO_2, the plane spacing is related to the lattice constant a, c, and Miller indices by the following formula

$$\frac{1}{d^3_{(hkl)}} = \frac{h^2+k^2}{a^2} + \frac{l^2}{c^2} \tag{3}$$

$$\sin^2\theta = \frac{\lambda^2}{4}\left(\frac{h^2+k^2}{a^2} + \frac{l^2}{c^2}\right) \tag{4}$$

According to the above formula, for the (1 1 0) orientation at $2\theta = 26.54^\circ$, the lattice constant a was calculated by

$$a = \frac{\lambda}{\sqrt{2}\sin\theta} \tag{5}$$

And for (0 0 2) orientation at $2\theta = 57.9^\circ$, the lattice constant c was calculated by

$$c = \frac{\lambda}{\sin\theta} \tag{6}$$

The lattice constants were determined as $a = 0.47466$ nm and $c = 0.31828$ nm for pure SnO_2. The calculated lattice constants a and c for Cd-doped SnO_2 nanorods are presented in Fig. 2c. For 3.0 wt% Cd-doped SnO_2, an increase in the lattice constants a and c (0.47677 and 0.31868 nm, respectively) would be expected when Sn^{4+} ions were replaced by Cd^{2+} ions due to mismatch in ionic radii.

To further study the structure of the nanorods, TEM and HRTEM combined with the SAED analysis techniques were employed. The typical TEM image of 3.0 wt% Cd-doped SnO_2 hierarchical nanostructures in Fig. 3a shows that the size and shape were similar to those of the FESEM observations. The HRTEM images of nanorods are showed in Fig. 3b and c, from which the clear lattice fringes were observed, indicating the high crystallinity of the nanorods. Different from the previous reports, in which 1 D SnO_2 grew along [1 0 1] direction [36], in our work the as-prepared nanorods were found to grow along two different directions. As shown in Fig. 3d, the lattice fringe spacing was observed to be 0.335 and 0.265 nm. Combined with the result of SAED (inset of Fig. 3b) analysis, they were found to correspond to (1 1 0) and (1 0 1) planes of rutile SnO_2, respectively. So, we could readily conclude that the present as-prepared Cd-doped SnO_2 nanorods actually grew along [1 $\bar{1}$ 2] direction. In Fig. 3e, the spacing between two adjacent horizontal and vertical lattice planes was 0.335 and 0.32 nm, which corresponded to (1 1 0) and (0 0 1) planes. The analysis result indicated a c-axis preferential growth direction. The same lattice parameters of these two kinds of nanorods with different growth direction had been obtained in previous report [35].

The gas sensing properties of hierarchical SnO_2 and the effect of Cd-doping on their sensitivity and selectivity were investigated. It is well known that the gas response is greatly influenced by the operating temperature and the amount of dopant [37,38]. In order to determine the optimum operating temperatures and doped amount, the responses of sensors using Cd-doped SnO_2 hierarchical nanostructures with different Cd amount to 10 ppm H_2S were tested as a function of operating temperature. For comparison, the response of the sensor based on undoped SnO_2 was also measured, as shown in Fig. 4a. It is obvious that undoped sensor had a poor response to H_2S, while the doped sensors with different amount of Cd exhibited higher response than the undoped one. Among all the Cd-doped SnO_2 sensors, the one with 3.0 wt% Cd showed the highest response to 10 ppm H_2S. Moreover, the response of all sensors varied with operating temperature. The response of sensors based on 3.0 and 5.0 wt% Cd doping increased rapidly and reached their maximum at the operating temperature of 275 °C, and then decreased with further increasing the operating temperature. The

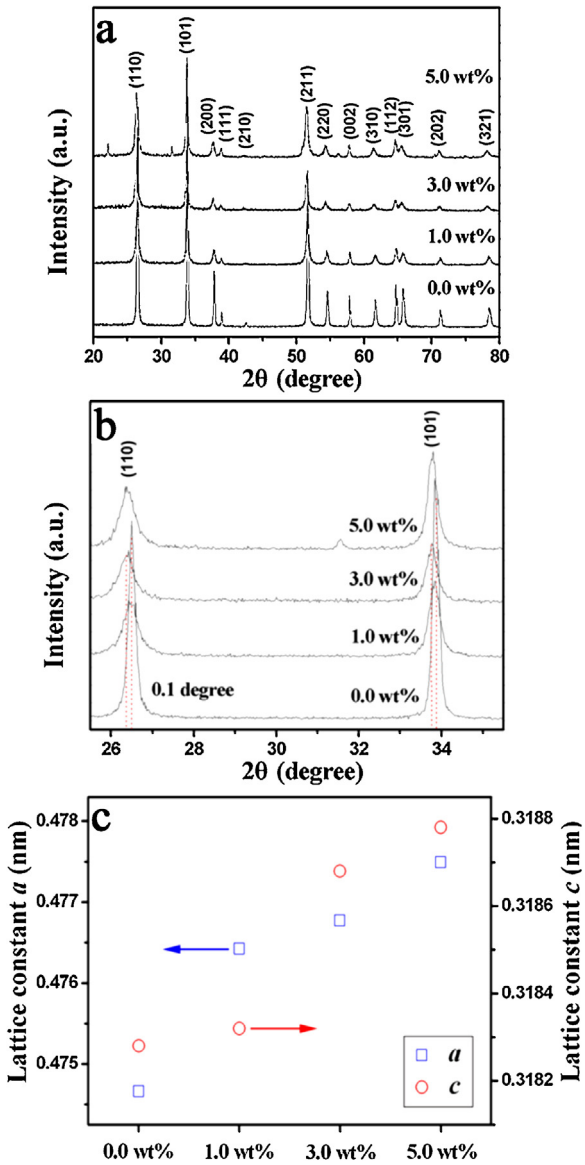

Fig. 2. (a) XRD patterns of samples with different amount of Cd. (b) Comparison of (1 1 0), and (1 0 1) peaks from XRD patterns. (c) Lattice constants of pure and Cd-doped SnO_2 nanorods.

undoped and 1.0 wt% Cd doped sensors had the maximum response at 250 °C. Based on the above results, it is found that the Cd-doped SnO_2 sensors displayed much better sensing properties than pure SnO_2 sensor. The optimum performance was obtained at 275 °C for the sensor based on 3.0 wt% Cd-doped SnO_2 hierarchical nanostructures. Therefore, all further measurements were carried out using this particular composition (3.0 wt%) and operating temperature (275 °C) to explore the effect of other factors on the sensing properties of Cd-doped SnO_2–H_2S. Fig. 4b shows the dependence of the resistances in air on the doping amount of Cd for the sensors at various temperatures. It can be seen that the resistances of all sensors decreased with increasing operating temperature, which was the intrinsic characteristic of a semiconductor. The doping of Cd brought about an increase in R_a and the increase trend of resistance was prominent. The increase in resistance in Cd-doped SnO_2 can be explained by the adsorption of oxygen species at surface oxygen vacancies. In terms of sensitivity, such high resistance values are favorable. However, it can negatively impact on the practical application of sensors.

For a gas sensor, selectivity is an important parameter. Fig. 5 shows a bar graph of the response of sensors based on undoped and 3.0 wt% Cd-doped SnO_2 nanorods to various testing gases, such as H_2S, H_2, methanol, acetone, and ethanol. All of the gases were tested at an operating temperature of 275 °C. It can be seen that the sensor based on pure SnO_2 nanorods exhibited an obvious response to ethanol, and less effective response to any other test gases. As expected, the sensor using 3.0 wt% Cd-doped SnO_2 nanorods displayed enhanced response for each gas compared with that based on undoped SnO_2 nanorods. By comparing the response behavior to various test gases, it is clearly found that Cd doping significantly improved the selectivity of the sensor. The response of sensor to H_2S was clearly higher than that to other gases. The highest response was about 31–10 ppm H_2S, which was about 22 times higher than that of the pure SnO_2. Consequently, it was concluded that the sensor using as-synthesized hierarchical 3.0 wt% Cd-doped SnO_2 nanorods showed good selectivity toward H_2S as opposed to any other gas at these concentrations.

The dynamic response characteristics of the sensor based on 3.0 wt% Cd-doped SnO_2 and pure SnO_2 hierarchical nanostructures to different reductive gases were investigated. Fig. 6a displays the response of the 3.0 wt% Cd-doped SnO_2 to 100 ppm C_3H_6O, C_2H_5OH, and 10 ppm H_2S at its corresponding optimal temperature of 275 °C, respectively. It is obvious that the sensor showed sensitive and reversible response to these gases. Moreover, compared with H_2S, the sensor exhibited the rapid response, and a nearly steady state was reached within minutes of exposure to C_3H_6O and C_2H_5OH. The response time was 15 and 10 s for C_3H_6O and C_2H_5OH, recovery time was 142 and 190 s, respectively. This almost square response

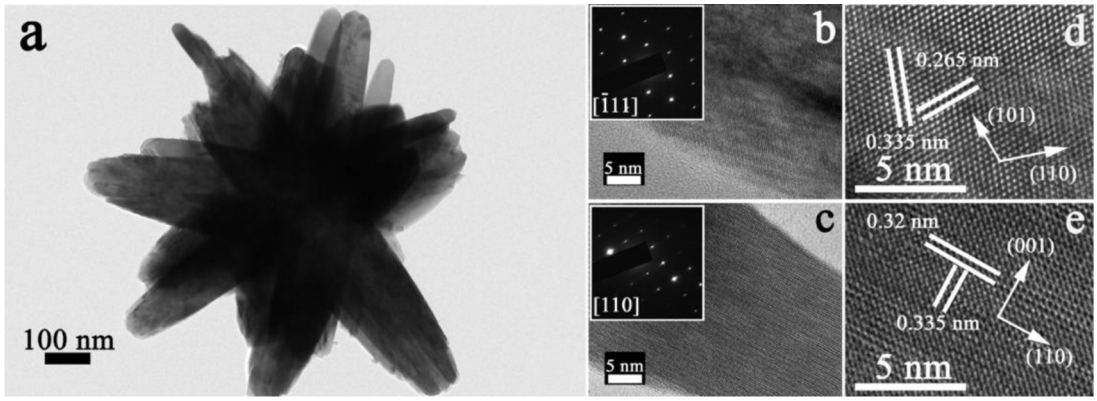

Fig. 3. (a) TEM and (b–e) HRTEM images of 3.0 wt% Cd-doped SnO_2 nanorods. The insets show the SAED parents.

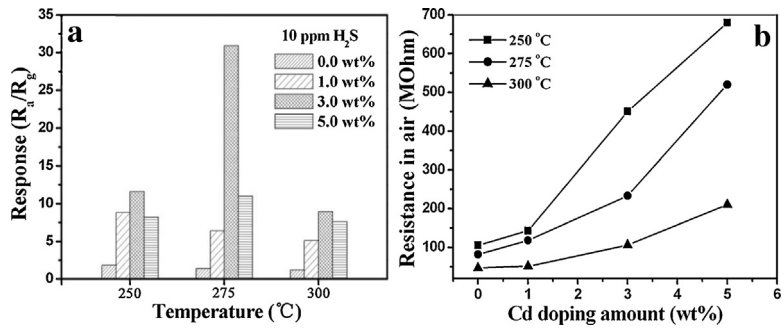

Fig. 4. (a) Response versus operating temperature of the sensors based on Cd-doped SnO_2 hierarchical nanostructures with different Cd amount exposing to 10 ppm H_2S at 275 °C. (b) The dependence of the resistances in air on the doping amount of Cd for the sensors at various temperatures.

shape observed indicated that the sensor first responded rapidly to acetone and ethanol, quickly achieving a near steady state [39]. Then the resistance of sensor changed slowly due to analyte gases diffusing through the material and occupying the remaining surface reaction sites. When the sensor was exposed to air, the resistance returned to the near baseline level. However, the response of the sensor to either C_2H_5OH or C_3H_6O was lower than that to H_2S even at a high concentration (100 ppm). Compared with the doped SnO_2 nanorods, the sensor based on pure SnO_2 displays the highest response to ethanol (Fig. 6b).

In order to study the effect of doping amount on the gas sensing properties of doped samples, the dependence of response on the doping amount was investigated. Fig. 7 shows the response of sensors based on hierarchical Cd-doped SnO_2 nanorods with different Cd amount versus the H_2S concentration ranging from 500 ppb to 10 ppm at 275 °C. Although the responses increased with increasing H_2S concentrations for three kinds of sensors, the response to H_2S for the 3.0 wt% Cd-doped SnO_2 sensor was obviously higher than that for the 1.0 and 5.0 wt% Cd-doped SnO_2 device, respectively. The inset of Fig. 7 indicates that the response almost linearly increased with increasing the gas concentration in the range from 500 ppb to 2 ppm for three sensors. As the H_2S concentration increased, the increase of the response of 3.0 wt% Cd-doped SnO_2 was faster. This suggested that the sensor based on Cd-doped SnO_2 (3.0 wt%) hierarchical nanostructures was more favorable to detect H_2S with low concentration.

The response characteristics and recovery characteristics were further investigated with the sensor using 3.0 wt% Cd-doped SnO_2 nanorods being orderly exposed to H_2S with different concentration at the operating temperature of 275 °C. It can be seen that the characteristics of response and recovery were almost reproducible, and a shark-fin-like profile was reached within minutes of exposure to H_2S, as shown in Fig. 8. The shark-fin response shape observed indicated that the sensor did not saturate during the measurement. On the other hand, there were a large number of surface sites suitable for reaction with H_2S. The response was about 2.1, 2.8, 5, 9.4, 17.6, 20.6 and 31 to 0.5, 1, 2, 5, 7, 8, and 10 ppm H_2S, respectively. A comparison between the sensing performances of the sensor and literature reports is summarized in Table 1. It is noteworthy that the sensor fabricated in our work exhibits better sensing performances compared with those reported in the literature [40–44].

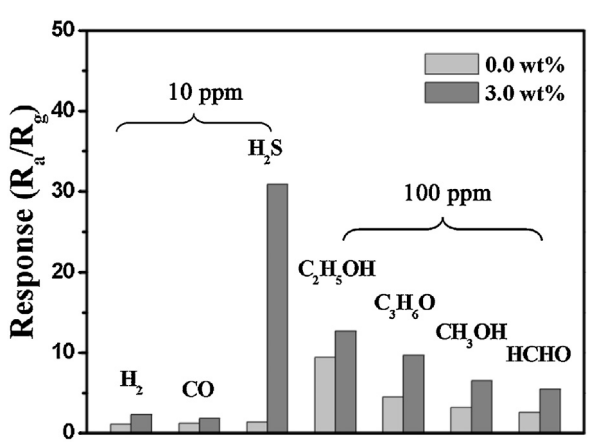

Fig. 5. Response of the sensor based on undoped and 3.0 wt% Cd-doped SnO_2 nanorods to different test gases at 275 °C.

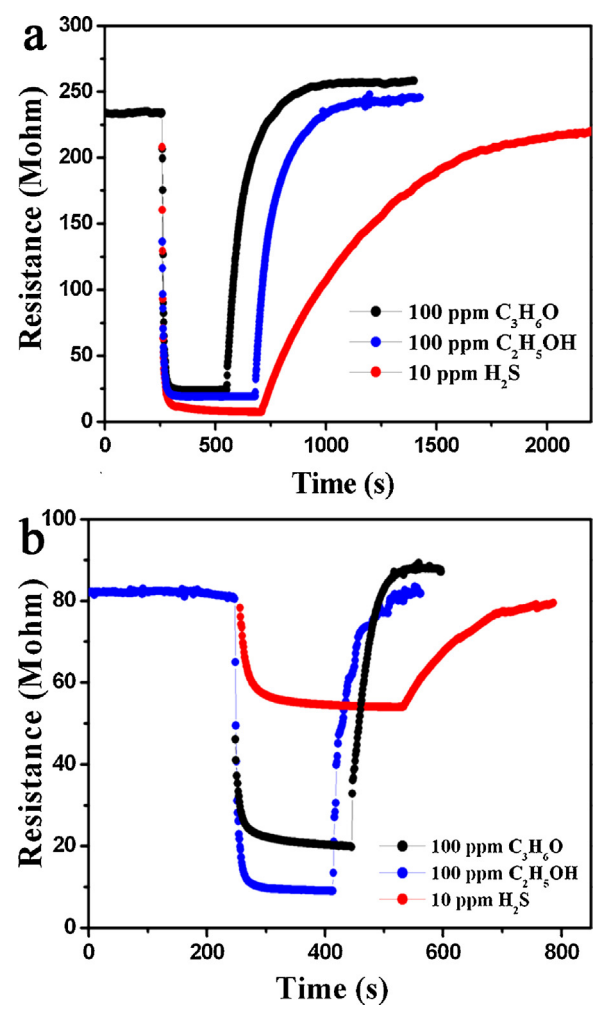

Fig. 6. Response transients of the sensors based on 3.0 wt% Cd-doped SnO_2 (a) and pure SnO_2 nanorods (b) to acetone, ethanol, and H_2S at 275 °C.

Table 1
Comparison of gas-sensing characteristics of gas sensors based on various SnO_2 nanostructures.

Material	Fabrication approach	H_2S concentration	Temperature (°C)	The formula of response	Sensor response	References
SnO_2/MoO_3 nanoparticles	Precipitation method	1 ppm	350	$(R_a-R_g)/R_a \times 100\%$	75%	[40]
CeO_2/SnO_2 nanoparticles	Sol–gel method	5 ppm	25	R_a/R_g	4	[41]
SnO_2 nanowires	Spray pyrolysis route	1.4 ppm	400	$(R_a-R_g)/R_a \times 100\%$	29%	[42]
SnO_2 nanorods	Solvothermal method	10 ppm	350	R_a/R_g	20	[43]
In_2O_3/SnO_2 nanotoasts	Precipitation method	10 ppm	300	R_a/R_g	4.98	[44]
Cd-SnO_2 hierarchical nanostructures	Hydrothermal route	1/10 ppm	275	R_a/R_g	2.8/31	This work

For the semiconductor oxide, the most widely accepted sensing mechanism [45–47] states that "when the sensor is exposed to air, oxygen molecules are adsorbed on the surface of the sensing materials, and ionized by electrons from the conduction band of materials to form chemisorbed oxygen species. As such, in this process, oxygen molecules act as electron acceptors only to result in the decrease of free electrons concentration in the materials conduction band and the increase of the measured resistance of the sensor. When the sensor is exposed to reductive gas atmosphere at a moderate temperature, surface reaction between the adsorbed oxygen species and gas molecules will occur. This process releases the trapped electrons back to the conduction band and leads to an increase of electron concentration, which results in a decrease in the resistance."

The ability of the sensing material to absorb and ionize oxygen species is fundamental to the performance of sensor. The dependence of sensitivity and selectivity on the doping amount can be mainly attributed to the changes of surface characteristics of the semiconductor oxides, which is induced by the modification effect of ions. As is well known, the sensitivity depends on the change of resistance in sensing body, which is derived from the reaction of the adsorbed oxygen species on the surface of semiconductor oxides with the test gas molecules, and that is the surface characteristic of semiconductor. Generally, the surface characteristics of semiconductor are closely related with its Fermi energy, surface oxygen vacancies, and the chemical shifts in binding energies of each element. In previous literature, the gas sensing mechanism of sensors based on Cd-doped SnO_2 nanostructures had been discussed [28–30]. In our work, XRD analysis results indicate that part of high valence Sn^{4+} ions are substituted by low valence Cd^{2+} ions. Based on solid state chemistry theory, the relatively higher concentration surface oxygen vacancies can be formed due to Cd^{2+} ions substitution, which is very important to the adsorption of oxygen on the surface of SnO_2 nanorods. On exposure to reducing gases, surface reaction between the adsorbed oxygen species and gas molecules will occur. In this case, reducing gas donates electrons back to SnO_2 conduction band. Therefore, the potential barrier in depletion region is decreased, leading to the increase in the conductance of sensor. This result can be considered to be a clue to understand the improved gas sensing properties due to Cd-doped in SnO_2. The enhancement in response to H_2S may be explained by the following reasons. According to previous literature [29,24], M-doping (M = Cd^{2+} and Cu^{2+}) can influence H_2S adsorption due to the difference in Pauling electronegativity between Cd (1.69), Cu (1.90) and Sn (1.96). The decrease in electronegativity leads to the increase in polarization of metal-oxygen bonds on the surface, which is favorable for H_2S adsorption. Moreover, in the presence of M-doping, H_2S adsorption will inject electronic states into the conduction band of SnO_2, which results in the change on the electrical conductivity of the surface of SnO_2. And it shows that M-doping improves the carrier release from H_2S to the sensor. As a result, the response of SnO_2 toward H_2S will be enhanced. In addition, this result is most likely to be connected with the catalytic effect of the Cd. Indeed, the catalytic effect of Cd as a means to enhance the sensitivity of SnO_2 sensors toward reducing gases is well known [28,48]. However, with the doping amount increasing to 5.0 wt%, the Cd^{2+} will combine with Sn^{4+} to form $CdSnO_3$ phase (Fig. 2a), which may prevent the formation of oxygen vacancies and lead to the decrease of quantity of oxygen vacancies in Cd-doped SnO_2 nanorods. As a result, the response of sensor (5.0 wt% Cd-doped SnO_2) to H_2S will decrease. Further study and systematic experiments are needed for the deep understanding of the doping-induced sensing properties, which is now in progress.

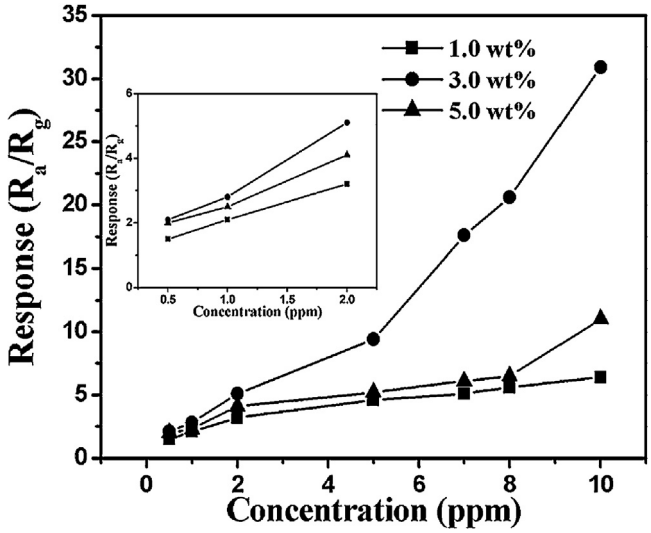

Fig. 7. Response of 1.0, 3.0, and 5.0 wt% Cd-doped SnO_2 hierarchical nanostructures versus H_2S concentrations at 275 °C.

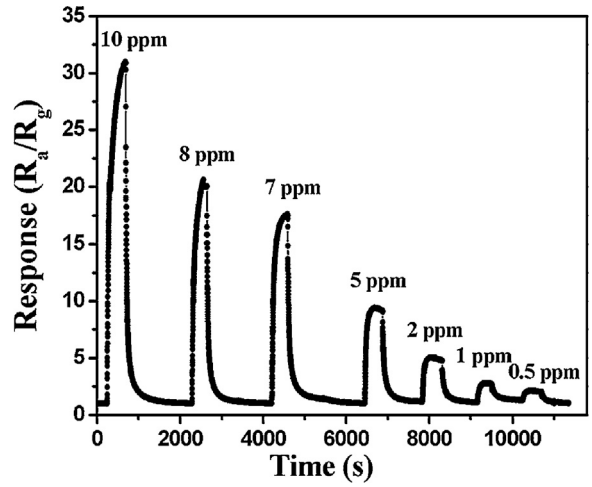

Fig. 8. Response transients of the 3.0 wt% Cd-doped SnO_2 hierarchical nanostructures to different concentration of H_2S at 275 °C.

4. Conclusions

In summary, the hierarchical unloaded and Cd-doped SnO_2 nanostructures had been synthesized by a simple one-step hydrothermal method. The results of characterization indicated that the hierarchical nanostructures were composed of many 1D nanorods. The hierarchical Cd-doped SnO_2 nanorods demonstrated significantly enhanced response to H_2S compared with their unloaded counterpart. Cd-doping could improve the formation of surface oxygen vacancy, which was probably responsible for the enhanced performance.

Acknowledgements

This work is supported by the National Nature Science Foundation of China (Nos. 61074172, 61134010, 60906036, and 61104203) and Program for Chang Jiang Scholars and Innovative Research Team in University (No. IRT1017). China Ministry of Public Security (No. 2011ZDYJJLST010). Project (20121105) Supported by Graduate Innovation Fund of Jilin University.

Appendix A. Supplementary data

Supplementary material related to this article can be found, in the online version, at http://dx.doi.org/10.1016/j.snb.2013.08.045.

References

[1] J. Kong, N.R. Franklin, C. Zhou, M.G. Chapline, S. Peng, K. Cho, H. Dai, Nanotube molecular wires as chemical sensors, Science 287 (2000) 622–625.
[2] A. Kolmakov, M. Moskovits, Chemical sensing and catalysis by one-dimensional metal-oxide nanostructures, Annu. Rev. Mater. Res. 34 (2004) 151–180.
[3] C. Hagleitner, A. Hierlemann, D. Lauge, A. Kimmer, N. Kerness, O. Brand, H. Baltes, Smart single-chip gas sensor microsystem, Nature 414 (2001) 293–296.
[4] Y. Cui, Q.Q. Wie, H.K. Park, C.M. Lieber, Nanowire nanosensors for highly sensitive and selective detection of biological and chemical species, Science 293 (2001) 1289–1292.
[5] Z.W. Pan, Z.R. Dai, Z.L. Wang, Nanobelts of semiconducting oxides, Science 291 (2001) 1947–1949.
[6] M. Law, H. Kind, B. Messer, F. Kim, P.D. Yang, Photochemical sensing of NO_2 with SnO_2 nanoribbon nanosensors at room temperature, Angew. Chem. Int. Ed. 41 (2002) 2405–2408.
[7] C. Li, D.H. Zhang, X.L. Liu, S. Han, T. Tang, J. Han, C.W. Zhou, In_2O_3 nanowires as chemical sensors, Appl. Phys. Lett. 82 (2003) 1613–1615.
[8] H.T. Wang, B.S. Kang, F. Ren, L.C. Tien, P.W. Sadik, D.P. Norton, S.J. Pearton, J. Lin, Hydrogen-selective sensing at room temperature with ZnO nanorods, Appl. Phys. Lett. 86 (2005) 243503.
[9] I. Heller, A.M. Janssens, J. Mannik, E.D. Minot, S.G. Lemay, C. Dekker, Identifying the mechanism of biosensing with carbon nanotube transistors, Nano Lett. 8 (2008) 591–595.
[10] N. Yamazoe, New approaches for improving semiconductor gas sensor, Sens. Actuators B 5 (1991) 7–19.
[11] F. Li, J.Q. Xu, X.H. Yu, L.Y. Chen, J.M. Zhu, Z.R. Yang, X.Q. Xin, One-step solid-state reaction synthesis and gas sensing property of tin oxide nanoparticles, Sens. Actuators B 81 (2002) 165–169.
[12] T. Sahm, L. Mädler, A. Gurlo, N. Barsan, S.E. Pratsinis, U. Weimar, Flame spray synthesis of tin dioxide nanoparticles for gas sensing, Sens. Actuators B 98 (2004) 148–153.
[13] A. Chowdhuri, V. Gupta, K. Sreenivas, R. Kumar, S. Mozumdar, P.K. Patanjali, Response speed of SnO_2-based H_2S sensors with CuO nanoparticles, Appl. Phys. Lett. 84 (2004) 1180–1182.
[14] T. Hyodo, S. Abe, Y. Shimizu, M. Egashira, Gas-sensing properties of ordered mesoporous SnO_2 and effects of coatings thereof, Sens. Actuators B 93 (2003) 590–600.
[15] Y.L. Wang, X.C. Jiang, Y.N. Xia, A solution phase precursor route to polycrystalline SnO_2 nanowires that can be used for gas sensing under ambient conditions, J. Am. Chem. Soc. 125 (2003) 16176–16177.
[16] G. Faglia, C. Baratto, G. Sberveglieri, M. Zha, A. Zappettini, Adsorption effects of NO_2 at ppm level on visible photoluminescence response of SnO_2 nanobelts, Appl. Phys. Lett. 86 (2005) 011923.
[17] P. Feng, X.Y. Xue, Y.G. Liu, Q. Wan, T.H. Wang, Achieving fast oxygen response in individual β-Ga_2O_3 nanowires by ultraviolet illumination, Appl. Phys. Lett. 89 (2006) 112114.
[18] D.H. Zhang, C. Li, X.L. Liu, S. Han, T. Tang, C.W. Zhou, Doping dependent NH_3 sensing of indium oxide nanowires, Appl. Phys. Lett. 83 (2003) 1845–1847.
[19] X.Y. Xue, Y.J. Chen, Y.G. Wang, T.H. Wang, Synthesis and ethanol sensing properties of $ZnSnO_3$ nanowires, Appl. Phys. Lett. 86 (2005) 233101.
[20] X.Y. Xue, L.L. Xing, Y.J. Chen, S.L. Shi, Y.G. Wang, T.H. Wang, Synthesis and H_2S sensing properties of CuO-SnO_2 core/shell PN-junction nanorods, J. Phys. Chem. C 112 (2008) 12157–12160.
[21] L.C. Tien, P.W. Sadik, D.P. Norton, L.F. Voss, S.J. Pearton, H.T. Wang, B.S. Kang, F. Ren, J. Jun, J. Lin, Hydrogen sensing at room temperature with Pt-coated ZnO thin films and nanorods, Appl. Phys. Lett. 87 (2005) 222106.
[22] A. Kolmakov, D.O. Kienov, Y. Liach, S. Stemmer, M. Moskovits, Enhanced gas sensing by individual SnO_2 nanowires and nanobelts functionalized with Pd catalyst particles, Nano Lett. 5 (2005) 667–673.
[23] G. Korotcenkov, Gas response control through structural and chemical modification of metal oxide films: state of the art and approaches, Sens. Actuators B 107 (2005) 209–232.
[24] W. Wei, Y. Dai, B.B. Huang, Role of Cu doping in SnO_2 sensing properties toward H_2S, J. Phys. Chem. C 115 (2011) 18597–18602.
[25] K. Jain, R.P. Pant, S.T. Lakshmikumar, Effect of Ni doping on thick film SnO_2 gas sensor, Sens. Actuators B 113 (2006) 823–829.
[26] P. Sun, L. You, Y.F. Sun, N.K. Chen, X.B. Li, H.B. Sun, J. Ma, G.Y. Lu, Novel Zn-doped SnO_2 hierarchical architectures: synthesis, characterization, and gas sensing properties, CrystEngComm 14 (2012) 1701–1708.
[27] X.H. Ding, D.W. Zeng, C.S. Xie, Controlled growth of SnO_2 nanorods clusters via Zn doping and its influence on gas-sensing properties, Sens. Actuators B 149 (2010) 336–344.
[28] T.S. Zhang, P. Hing, L. Yang, J.C. Zhang, Selective detection of ethanol vapor and hydrogen using Cd-doped SnO_2-based sensors, Sens. Actuators B 60 (1999) 208–215.
[29] R.H.R. Castro, P. Hidalgo, H.E.M. Perez, F.J. Ramirez-Fernandez, D. Gouvêa, Relationship between surface segregation and rapid propane electrical response in Cd-doped SnO_2 nanomaterials, Sens. Actuators B 133 (2008) 263–269.
[30] X.C. Zhang, H.M. Yang, Structural characterization and gas sensing property of Cd-doped SnO_2 nanocrystallites synthesized by mechanochemical reaction, Sens. Actuators B 173 (2012) 127–132.
[31] P. Sun, W.N. Wang, Y.P. Liu, Y.F. Sun, J. Ma, G.Y. Lu, Hydrothermal synthesis of 3 D urchin-like α-Fe_2O_3 nanostructure for gas sensor, Sens. Actuators B 173 (2012) 52–57.
[32] P. Sun, X.X. He, W.B. Wang, J. Ma, Y.F. Sun, G.Y. Lu, Template-free synthesis monodisperse α-Fe_2O_3 porous ellipsoids and their application to gas sensors, CrystEngComm 14 (2012) 2229–2234.
[33] H.T. Fan, Y. Zeng, H.B. Yang, X.J. Zheng, L. Liu, T. Zhang, Preparation and gas sensitive properties of ZnO–CuO nanocomposites, Acta Phys. Chem. Sin. 24 (2008) 1292–1296.
[34] A. Tricoli, M. Graf, S.E. Pratsinis, Optimal doping for enhanced SnO_2 sensitivity and thermal stability, Adv. Funct. Mater. 18 (2008) 1969–1976.
[35] D.F. Zhang, L.D. Sun, J.L. Yin, C.H. Yan, Low-temperature fabrication of highly crystalline SnO_2 nanorods, Adv. Mater. 12 (2003) 1022–1025.
[36] L.B. Fraigi, D.G. Lamas, N.E. Walsöe de Reca, Comparison between two combustion routes for the synthesis of nanocrystalline SnO_2 powders, Mater. Lett. 47 (2001) 262–266.
[37] V.R. Shinde, T.P. Gujar, C.D. Lokhande, Enhanced response of porous ZnO nanobeads towards LPG: effect of Pd sensitization, Sens. Actuators B 123 (2007) 701–706.
[38] Z. Cao, J.R. Stetter, A selective solid-state gas sensor for halogenated hydrocarbons, Sens. Actuators B 5 (1991) 109–113.
[39] S.C. Naisbitt, K.F.E. Pratt, D.E. Williams, I.P. Parkin, A microstructural mode of semiconducting gas sensor response: the effects of sintering temperature on the response of chromium titanate (CTO) to carbon monoxide, Sens. Actuators B 114 (2006) 969–977.
[40] S.C. Lee, S.Y. Kim, B.W. Hwang, S.Y. Jung, D. Ragupathy, I.S. Son, D.D. Lee, J.C. Kim, Improvement of H_2S sensing properties of SnO_2-based thick film gas sensors promoted with MoO_3 and NiO, Sensors 13 (2013) 3889–3901.
[41] G.J. Fang, Z.L. Liu, C.Q. Liu, K.L. Yao, Room temperature H_2S sensing properties and mechanism of CeO_2–SnO_2 sol–gel thin film, Sens. Actuators B 66 (2000) 46–48.
[42] E. Brunet, T. Maier, G.C. Mutinati, S. Steinhauer, A. KöcK, C. Gspan, W. Grogger, Comparison of the gas sensing performance of SnO_2 thin film and SnO_2 nanowire sensors, Sens. Actuators B 165 (2012) 110–118.
[43] J.Q. Xu, D. Wang, L.P. Qin, W.J. Yu, Q.Y. Pan, SnO_2 nanorods and hollow spheres: controlled synthesis and gas sensing properties, Sens. Actuators B 137 (2009) 490–495.
[44] D.W. Chu, Y.P. Zeng, D.L. Jiang, Y. Masuda, In_2O_3–SnO_2 nano-toasts and nanorods: precipitation preparation, formation mechanism, and gas sensitive properties, Sens. Actuators B 137 (2009) 630–636.
[45] N. Yamazoe, G. Sakai, K. Shimanoe, Oxide semiconductor gas sensor, Catal. Surv. Asia 7 (2003) 63–75.
[46] M. Egashira, Y. Shimizu, Y. Takao, S. Sako, Variations in I–V characteristics of oxide semiconductors induced by oxidizing gases, Sens. Actuators B 35 (1996) 62–67.
[47] N.J. Dayan, S.R. Sainkar, R.N. Karekar, R.C. Aiyer, Formulation and characterization of ZnO:Sb thick-film gas sensor, Thin Solid Films 325 (1998) 254–258.
[48] J. Mizsei, V. Lantto, Simultaneous response of work function and resistivity of some SnO_2-based samples to H_2 and H_2S, Sens. Actuators B 4 (1991) 163–168.

Biographies

Peng Sun received his MS degree from State Key Laboratory of Superhard Materials, Jilin University, China in 2009. He entered the PhD course in 2010, majoring in microelectronics and solid state electronics. Now, he is engaged in the synthesis and characterization of the semiconducting functional materials and gas sensors.

Xin Zhou received his BS degree from the Electronics Science and Engineering Department, Jilin University, China in 2013. Presently, he is a graduate student, majored in microelectronics and solid state electronics.

Chen Wang received his BS degree from the Electronics Science and Engineering Department, Jilin University, China in 2013. Now, he is a graduate student, majored in microelectronics and solid state electronics.

Biao Wang obtained his PhD degree from Jilin University, China in 2008. Now he is a research professor in Changchun Institute of Optics, Fine Mechanics and Physics, Chinese Academy of Science. His current research is laser gas sensor.

Xiumei Xu received her MS degree from college of chemistry, Jilin University, China. She entered the PhD course in 2011, majoring in microelectronics and solid state electronics. Now, she is engaged in the synthesis and characterization of the semiconducting functional materials and gas sensors.

Geyu Lu received his BS and MS degree in electronic sciences from Jilin University, China in 1985 and 1988, respectively, and PhD degree in 1998 from Kyushu University in Japan. Now he is a professor of Jilin University, China. Presently, he is interested in the development of functional materials and chemical sensors.